HHS Public Access

Author manuscript

Exp Neurol. Author manuscript; available in PMC 2022 February 18.

Published in final edited form as:

Exp Neurol. 2020 October ; 332: 113388. doi:10.1016/j.expneurol.2020.113388.

Aged heterozygous *Cdkl5* mutant mice exhibit spontaneous epileptic spasms

Patrick J. Mulcahey[a,1], **Sheng Tang**[a,b,1], **Hajime Takano**[a,1], **Alicia White**[a], **Dayana R. Davila Portillo**[a], **Owen M. Kane**[a], **Eric D. Marsh**[a,c], **Zhaolan Zhou**[d], **Douglas A. Coulter**[a,b,*]

[a]Division of Child Neurology and CHOP Research Institute, Children's Hospital of Philadelphia, United States of America

[b]Department of Neuroscience and Pediatrics, University of Pennsylvania Perelman School of Medicine, United States of America

[c]Departments of Neurology, and Pediatrics, University of Pennsylvania Perelman School of Medicine, United States of America

[d]Department of Genetics, University of Pennsylvania Perelman School of Medicine, United States of America

Abstract

CDKL5 deficiency disorder (CDD) is a devastating neurodevelopmental disorder characterized by early-onset epilepsy, severe intellectual disability, cortical visual impairment and motor disabilities. Epilepsy is a central feature of CDD, with most patients having intractable seizures, but seizure frequency and severity can vary. Clinical reports demonstrate a diversity in seizure semiology and electrographic features, with no pattern diagnostic of CDD. Although animal models of CDD have shown evidence of hyperexcitability, spontaneous seizures have not been previously reported. Here, we present the first systematic study of spontaneous seizures in mouse models of CDD. Epileptic spasms, the most frequent and persistent seizure type in CDD patients, were recapitulated in two mouse models of CDD carrying heterozygous mutations, *Cdkl5*^{R59X} and *Cdkl5*^{KO}. Spasm-like events were present in a significant proportion of aged heterozygous female mice carrying either of the two *Cdkl5* mutations with significant variability in seizure burden. Electrographically, spasms were most frequently associated with generalized slow-wave activity and tended to occur in clusters during sleep. CDD mice also showed interictal and background abnormalities, characterized by high-amplitude spiking and altered power in multiple frequency bands. These data demonstrate that aged female heterozygous *Cdkl5* mice recapitulate multiple features of epilepsy in CDD and can serve to complement existing models of epileptic spasms in future mechanistic and translational studies.

*Corresponding author at: Rm. 410D Abramson Pediatric Research Building, 3516 Civic Blvd., Philadelphia, PA 19104, United States of America. coulterd@email.chop.edu (D.A. Coulter).

[1]These authors contributed equally to this work.

Author contributions

P.J.M, S.T., H.T, E.D.M., Z.Z., and D.A.C. designed the experiments and reviewed and analyzed the data. A.W., D.R.D.P., and O.M.K. assisted with experiments and data interpretation. S.T. and P.J.M. wrote the manuscript with input from all other authors.

Declaration of Competing Interest

The authors declare no competing financial interests.

Supplementary data to this article can be found online at https://doi.org/10.1016/j.expneurol.2020.113388.

Keywords

CDKL5; Epilepsy; Epileptic spasms; Neurodevelopmental disorders

1. Introduction

CDKL5 deficiency disorder (CDD) is a rare but devastating neurodevelopmental disorder characterized by early-onset epilepsy, intellectual disability, cortical visual impairments, and motor disabilities (Demarest et al., 2019; Olson et al., 2019). It is caused by loss-of-function mutations in the X-linked gene, cyclin-dependent kinase-like 5 (*CDKL5*) and occurs with an estimated prevalence of 1 in 40,000 births (Symonds et al., 2019). The majority of patients are heterozygous females, with fewer hemizygous males reported (Demarest et al., 2019; Fehr et al., 2016; Olson et al., 2019). With rising awareness of CDD and the incorporation of *CDKL5* into genetic screening panels, CDD is increasingly recognized as a significant cause of early-onset epilepsy and neurodevelopmental disorders. In select cohorts of patients with early-onset epilepsy, *CDKL5* has been reported as one of the most common genetic diagnoses, after genes such as *SCN1A* and *KCNQ2* (Butler et al., 2017; Lindy et al., 2018; Symonds et al., 2019).

Seizures are almost always the presenting problem in CDD. The vast majority of CDD patients experience seizures, with a median age of onset at 6 weeks (Bahi-Buisson et al., 2008b; Fehr et al., 2016). Although natural history studies of CDD have been limited by the small number of patients, some have reported a three-stage progression of epilepsy in CDD (Bahi-Buisson et al., 2008a). The first stage is usually characterized by the onset of generalized tonic-clonic seizures with a normal background EEG, and it is followed by a brief seizure-free “honeymoon” period in some patients. The second stage, termed “epileptic encephalopathy,” features infantile spasms with hypsarrhythmia and other background EEG abnormalities. The third stage is highly variable: most patients progress to multifocal, treatment-refractory epilepsy, whereas a minority of patients become seizure-free on poly-therapy. Importantly, case studies in recent years have highlighted the heterogeneous nature of seizures in CDD, with reports of myoclonic seizures, hypermotor-tonic spasms, and reflex seizures (Demarest et al., 2019; Klein et al., 2011; Pintaudi et al., 2008; Takeda et al., 2020). These seizures correlate with a diverse range of electrographic findings, including ictal as well as interictal abnormalities (Demarest et al., 2019; Fallah and Eubanks, 2020).

To date, the mechanisms underlying the heterogeneity of seizures in CDD remain unclear. Several mouse models of CDD have been generated (Amendola et al., 2014; Okuda et al., 2018; Tang et al., 2019; Wang et al., 2012). Although *Cdkl5* knockout mice demonstrate features of hyperexcitability at the circuit level, they do not appear to have spontaneous seizures at up to 4 months of age (Amendola et al., 2014; Okuda et al., 2017; Wang et al., 2012). Similarly, seizure threshold studies using chemoconvulsants have yielded mixed results (Amendola et al., 2014; Okuda et al., 2017).

Here, we report, for the first time, recurrent spontaneous seizures in aged heterozygous female mice in two distinct models of CDD, $Cdkl5^{R59X}$/+ and $Cdkl5^{KO}$/+ (Tang et al., 2019; Wang et al., 2012). Epileptic spasms were the major spontaneous seizure type, characterized

by sudden-onset body spasm typically associated with generalized slow-wave activity on EEG, with variable presence of electrodecrement. Similar to epileptic spasms in CDD and other seizure disorders, these spasms tended to occur in clusters and were more frequent during periods of heightened delta power during slow-wave sleep (Bernardo et al., 2019). *Cdkl5* mutant mice also showed significant interictal abnormalities, characterized by high-amplitude, generalized spiking. Finally, power spectral analysis revealed distinct features of background EEG in *Cdkl5* mutant mice. Taken together, our study represents the first report of epilepsy in an animal model of CDD, establishing the potential of aged female *Cdkl5* mutant mice for future mechanistic and translational studies of CDD-related epilepsy and epileptic spasms.

2. Materials and methods

2.1. Mouse strains

The CDKL5 R59X knock-in (*Cdkl5*^{R59X}) (Tang et al., 2019) and *Cdkl5* knockout (*Cdkl5*^{KO}) (Wang et al., 2012) lines, which are also available from Jackson Laboratories (*Cdkl5*^{R59X}: Stock No. 028856; *Cdkl5*^{KO}: Stock No. 021967), were obtained as a generous gift from the Zhou Lab at the University of Pennsylvania. Briefly, colonies of *Cdkl5*^{R59X} and *Cdkl5*^{KO} mice were maintained by breeding heterozygous female breeders from each line (*Cdkl5*^{R59X}/+ or *Cdkl5*^{KO}/+) to wild type C57BL/6 J mice. The resulting mutant female offspring (*Cdkl5*^{R59X}/+ or *Cdkl5*^{KO}/+) and their respective wild type littermates (+/+), were used for experiments.

2.2. Animal husbandry

Experiments were conducted in accordance with the ethical guidelines of the National Institutes of Health and with the approval of the Institutional Animal Care and Use Committee of the University of Pennsylvania and the Children's Hospital of Philadelphia's Institutional Animal Care and Use Committee. All methods were in accordance with the relevant guidelines and regulations. Mice were group-housed in cages of two to five in a twelve-hour light/dark cycle with food and water provided ad libitum. All progeny was genotyped either with the previously reported PCR strategies or with quantitative PCR by Transnetyx, Inc. (Tang et al., 2019; Wang et al., 2012). Heterozygous female littermates (+/+, *Cdkl5*^{R59X}/+, *Cdkl5*^{KO}/+) were weaned at 3 weeks of age and housed together. After EEG electrode implantation surgery, mice were individually housed and kept on a 12 h light/dark cycle with ad libitum access to food and water.

2.3. Four-channel EEG implantation surgery

Experiments were conducted in accordance with the approval of the Institutional Animal Care and Use Committee of the Children's Hospital of Philadelphia. EEG recording was performed as previously described (Kahn et al., 2019). Mice were stereotaxically implanted with an electrode assembly under continuous isoflurane anesthesia. The electrode assembly consisted of 6 leads: 2 surface electrodes attached to miniature skull screws placed over the left and right frontal cortices (from Bregma: A/P − 1.2 mm, M/L ± 1.1 mm); a double-depth electrode in right hippocampus (A/P − 2.2 mm, M/L + 1.2 mm, D/V − 1.3 mm); and finally a reference and a ground electrode directly behind Lambda on either side of midline. Teflon-

coated silver wires (0.13 mm diameter) were attached to each electrode and connected to a 6-pin pedestal (Plastics One, Roanoke, VA). The entire assembly was secured on the skull with dental cement (Ortho-Jet, Lang Dental, Wheeling, IL). All surgeries were performed by an experimenter blinded to genotype.

2.4. Eight-channel EEG implantation surgery

Electroencephalographic mouse studies were performed as previously described (Marsh et al., 2009; Simonet et al., 2015). The implant procedure, under ketamine/xylazine and isoflurane anesthesia, consisted of the stereotaxic placement of 8 electrodes (hippocampal, bilateral parietal, bilateral motor, bilateral visual electrodes) using the following coordinates (from Bregma – Bilateral motor: 0.5 mm Anterior-Posterior (A-P) and 1.0 mm medial-lateral (M-L); bilateral parietal: −0.7 mm A-P, 3.0 mm M-L; bilateral visual −3.5 A-P, 2.0 mm M-L; hippocampus: −2.2 mm A-P, 2.0 mm M-L, and 1.7 mm ventral). All electrodes were produced by attaching 125 μM silver wire (78,600, A-M Systems) to a 10-channel Omnetics nanoconnector (AP8393–001, Omnetics Corp). Electrodes were placed after drilling 1 mm (0.6 mm Drill Bit cat no.39416022 Lecia) holes at each stereotaxic location, with cortical electrodes placed at the superficial cortical surface. The electrodes were covered with dental cement which attached the connector to the head. After 24–48 h of recovery in their home cage the animals were transferred to the monitoring cage and recorded using a 32-channel Intan extracellular amplifier (RHD2000 USB Interface Board, Intan Technologies) using either DataWave software or importing the raw data into Matlab. The recordings were sampled at 2000 Hz, with no on-line filtering. Electrode impedances were tested prior to all recordings. All animals were recorded for at least 72 h.

2.5. Video-EEG recording

A flexible cable connected each animals headcap assembly to a commutator thus allowing the mouse to move freely during the recordings. Mice were given at least 72 h post-surgery to recover prior to being placed in a recording cage and were acclimatized for at least 72 h before recording initiation. Video-monitored EEG recordings of awake and behaving mice were performed in custom-made Plexiglas cages using a Stellate Harmonie acquisition interface (Natus Medical, Pleasanton, CA) and sampled at 200 Hz in a 12-h light/dark cycle with food and water provided ad libitum. Wild type, *Cdkl5*^{R59X}/+, and *Cdkl5*^{KO}/+ mice were randomized and placed into cohorts of four individual cages monitored by a single video camera, and each grouped cohort underwent video-EEG recording during the same period. All experimenters were blinded to genotype throughout the video-EEG recording process.

2.6. Video-EEG data interpretation

All video-EEG interpretation and analysis were performed by an experimenter blinded to genotype. EEG signals were reviewed in Stellate Browser (Stellate Systems, Inc., Montreal, Canada). For each animal, three consecutive days of 24 h EEG monitoring from Day 7 – Day 11 relative to the beginning of the recording period were randomly selected and reviewed by a blinded reviewer.

2.7. Manual seizure detection

Prior to analysis, all EEG traces were pre-processed with the application of a 0.1 Hz high-pass filter, 70 Hz low-pass filter, and 60 Hz notch filter. Cortical channels were viewed at a scale 30–75 μV/mm, and hippocampal channels were viewed at a scale of 30–50 μV/mm. Sixty seconds of EEG were viewed in each frame. A blinded reviewer systematically screened the entirety of each EEG trace for large-amplitude, bilaterally synchronous slow-wave, spike-wave, sharp-wave, polyspike-wave, or spike/sharp activity. For each EEG event, time-locked video was used to assess for the presence of motor activity. Motor activity was considered typical of an epileptic spasm if it was 1) sudden-onset during a period of relative immobility, 2) a single, brief spasm involving limbs and/or trunk, and 3) temporally time-locked with the ictal event of interest (i.e. occurring concurrently with or immediately after the onset of the waveform). Only events with both typical ictal EEG waveforms and motor activity were considered epileptic spasms. Three days of EEG were reviewed to determine the presence or absence of spasms (for days without spasms, the entire 24 h period was examined). For animals that showed spasms on more than one of the three days reviewed, one day was randomly selected, and the total number of spasms was quantified by a reviewer.

2.8. Automated seizure detection

We adopted a previously published detector for synchronous spiking (Ahrens-Nicklas et al., 2019). We applied this detector to a 24 h period of EEG for each mouse in our study during Day 8 relative to the start of recording. This spike detection algorithm examined non-overlapping 5 min segments of intracranial EEG data from bilateral cortical screws. The segments were initially notch filtered at 60 Hz and bandpass filtered from 1 to 70 Hz. An initial amplitude threshold of 300 μV was applied to ensure that we only captured high-amplitude spiking events. We then applied a 5-standard deviation threshold to the absolute value of the 5 min segment to screen for spikes. Peaks found within 0.025 s (5 samples) of each other were considered to be the same event. Video was not used to curate events captured by this algorithm. We thank Rebecca Ahrens-Nicklas for their validated code structure, which we modified for this analysis.

2.9. Background EEG analysis

EEG signals were processed offline for the purpose of power spectral density analyses. Power spectral analyses were performed using custom written MATLAB code. For all analyses, frequency bands were separated into delta (0.1–4 Hz), theta (4–8 Hz), alpha (8–13 Hz), beta (13–25 Hz), and gamma (25–50 Hz) ranges. The relative power for each frequency band was calculated by dividing the absolute power for each frequency by the total power and then normalizing it with a log transformation to allow comparisons between mice. To examine changes in power spectral density associated with seizure clusters, power spectral analysis was performed during a 24 h period on one cortical and one hippocampal channel, using epochs of five minutes. For assessment of the correlation between delta power and spasm occurrence, delta power values in one hippocampal channel across a 24 h period for each mouse was transformed to a list of z-scores. Each z-score was calculated as $(x - \mu) / \sigma$, where x is delta power for a specific epoch, μ is the overall mean delta power during the

enclosing 24 h period, and σ is the sample standard deviation of the delta power during the 24 h period. The distribution of z-scores during spasms was then compared to the overall distribution of delta power during the enclosing 24 h period. To assess overall differences in background power between wild type and *Cdkl5* mutant mice, ten ten-minute segments were randomly sampled and analyzed from each of the light and dark cycles from Day 8 relative to the start of recording. We modified the analysis, including fast Fourier transforms (FFTs), from a previous publication (Ahrens-Nicklas et al., 2019). Our custom MATLAB code can be found on Github (https://github.com/mulcaheyp/cdkl5_2020).

2.10. Statistical analysis

Because this is the first systematic study of spontaneous seizures in mouse models of CDD, no estimate of spontaneous seizure incidence or frequency was available in literature. We pre-determined our sample size at approximately 8 mice per genotype, which would be sufficient to detect epilepsy in multiple mice as long as the incidence was at least 25% in each of the mutant lines. Statistical analyses were performed using Prism (GraphPad). All data sets were analyzed using the Shapiro-Wilk test for normality. Data sets with normal distributions were analyzed for significance using the unpaired Students *t*-test, whereas data sets with non-normal distributions were analyzed using the Mann-Whitney test. For comparisons of spasm occurrence and spasm burden, one-tailed Mann-Whitney tests were performed with Holm's correction for multiple comparisons. For power spectral analysis, two-way ANOVA was performed with Dunnett's multiple comparisons test. Graphs are plotted using Prism (GraphPad). In our figures, *p*-values between 0.05 and 0.1 are shown explicitly, * is used to denote all $0.01 < p < .05$, ** for $0.001 < p < .01$, *** for $0.0001 < p < .001$, and **** for $p < .0001$.

3. Results

3.1. Aged female Cdkl5 heterozygous mice exhibit epileptic spasms

Multiple previous studies in male hemizygous *Cdkl5* mutant mice have failed to show epilepsy in mice younger than 4 months of age (Amendola et al., 2014; Okuda et al., 2017; Wang et al., 2012). These studies also conducted behavioral assays in both male and female *Cdkl5* mutant mice, and despite extensive handling and observation, no seizure-like behavior has been observed. Recently, there have been anecdotal reports of reflex seizures, provoked by handling, in aged female *Cdkl5* mice by 42 weeks of age (unpublished data, laboratory of Zhaolan Zhou). Therefore, we reasoned that spontaneous seizures may also be occurring along a similar timeline. We monitored, using concurrent video and four-channel electroencephalography (video-EEG) recording, a cohort of > 300-day old heterozygous female *Cdkl5* mutant mice and wild type littermates (Supplementary Table 1). To improve the generalizability of our findings, we incorporated heterozygous female mutant mice from two distinct models of CDD, $Cdkl5^{R59X}/+$ (a patient missense mutation) and $Cdkl5^{KO}/+$ (a patient splice site mutation), both of which have been characterized as loss-of-function alleles (Tang et al., 2019; Wang et al., 2012). In the majority of $Cdkl5^{R59X}/+$ (6/7, or 86%) and $Cdkl5^{KO}/+$ (6/9, or 67%) mice, we observed a high frequency of epileptic spasms (Fig. 1, Supplementary videos 1 and 2, Supplementary Fig. 1). These events were characterized by sudden-onset, brief spasms involving the limbs or trunk and were most commonly

associated with high-amplitude slow-wave activity (200–500 ms) on EEG. However, there was variability in the ictal waveform, which occasionally appeared as spike (< 70 ms)-wave, sharp (70–200 ms)-wave, or polyspike-wave activity. Electrodecrement, or voltage attenuation immediately following the ictal event, was variably present. The severity of the spasms often correlated with the amplitude of the epileptiform activity on EEG, with some spasms causing loss of balance with impairment of the righting reflex for a few seconds. Over at least 3 days of video-EEG monitoring for each of 16 *Cdkl5* mutant mice, epileptic spasms were the only type of spontaneous seizure we consistently observed.

3.2. Epileptic spasms in Cdkl5 mutant mice are generalized in nature

In human patients, epileptic spasms are often characterized by spike-wave or slow-wave activity that can be generalized or focal-onset in nature (Bahi-Buisson et al., 2008a, 2008b; Kellaway et al., 1979). We therefore asked if individual *Cdkl5* mutant mice demonstrated a specific focality in the patterns of epileptiform discharges. We conducted eight-channel EEG with concurrent video monitoring in a small cohort of *Cdkl5* mutant mice, with recording electrodes in the bilateral motor, barrel, and visual cortices, in addition to depth electrodes in the bilateral hippocampi. In $Cdkl5^{KO}$/+ mice, we captured similar epileptic spasms as those observed on four-channel EEG (Fig. 2). All of the ictal events we reviewed in our eight-channel recordings ($n = 2$ $Cdkl5^{KO}$/+ mice) showed bilaterally symmetric onset, suggesting that spasm-associated EEG events in these mice are likely of a generalized nature.

3.3. Cdkl5 mutant mice show heterogeneity in seizure burden

To estimate seizure burden across our cohort of mutant mice, we employed a trained, blinded reviewer to screen for spasms over three consecutive days of video-EEG monitoring, applying the criteria of a significant ictal event on EEG occurring in a time-locked manner with an observed motor spasm on video (Materials and Methods). We reviewed three days of continuous video-EEG data for each of 8 control (+/+), 7 $Cdkl5^{R59X}$/+, and 9 $Cdkl5^{KO}$/+ mice. In comparison to wild type controls, $Cdkl5^{R59X}$/+ and $Cdkl5^{KO}$/+ mice showed significantly increased numbers of days with spasms.

To estimate the daily spasm burden, we counted the number of spasms in a 24 h period for each mouse. For mice with multiple days of spasms, one day was randomly selected and counted. Interestingly, despite having a homogeneous genetic background and being similar in age (Supplementary Table 1), $Cdkl5^{R59X}$/+ and $Cdkl5^{KO}$/+ mice showed significant heterogeneity in seizure burden (Fig. 3), with some mice having over 100 spasms per day.

In addition to our blinded manual review of EEG, we attempted to quantify spasm-associated EEG events in an automated manner. We employed a published algorithm that detects spiking activity based on synchrony across channels (Ahrens-Nicklas et al., 2019). This approach yielded findings that showed a trend toward increased spikes in $Cdkl5^{R59X}$/+ and $Cdkl5^{KO}$/+ mice, with average values for events per day that were similar to those obtained from manual detection (Supplementary Fig. 2). However, this approach also suffered from a significant number of false positives, particularly in certain wild type mice, and the result did not show a statistically significant difference in ictal

events across the genotypes. This may be related to the observation that slow-wave activity in *Cdkl5* mutant mice shown significant variation in amplitude, duration, and waveform morphology (Supplementary Fig. 1), with the lack of a single, stereotypical waveform making it challenging for an automated detector to consistently capture ictal events.

3.4. Spasms occur in clusters during periods of slow-wave sleep

Epileptic spasms in human patients are known to occur in clusters and be associated with specific phases of the sleep-wake cycle (Kellaway et al., 1979). These are also considered to be important features in establishing animal models of epileptic spasms (Dulla, 2018; Marsh and Golden, 2009). Similarly, sleep-related seizures have been frequently reported in CDD (Bernardo et al., 2019; Grosso et al., 2007). In *Cdkl5*^{R59X}/+ and *Cdkl5*^{KO}/+ mice, we observed that epileptic spasms occur in both the light and dark cycles, but they tended to occur in clusters during periods of quiet immobility. Clusters of spasms appeared to be associated with a characteristic background EEG of elevated delta power suggestive of slow-wave sleep (Fig. 4). Next, we assessed this association quantitatively in a subset of *Cdkl5*^{R59X}/+ and *Cdkl5*^{KO}/+ mice with high seizure burden (n = 3 per genotype). For each mouse, we calculate delta power values in five-minute epochs over a 24 h period and standardized these values as z-scores. We then compared the distribution of z-scores during spasms to the distribution of z-scores over the enclosing 24 h period. In both *Cdkl5*^{R59X}/+ and *Cdkl5*^{KO}/+ mice, we found that delta power during spasms was significantly shifted toward higher values.

3.5. Cdkl5 mutant mice show interictal and background abnormalities

Interictal abnormalities, such as generalized spikes and spike-wave activity, have been frequently reported in CDD (Bahi-Buisson et al., 2008a, 2008b; Fallah and Eubanks, 2020). During our review of video-EEG recordings of *Cdkl5*^{R59X}/+ and *Cdkl5*^{KO}/+ mice, we observed similar interictal features, characterized by high-amplitude, bilaterally synchronous spikes occurring during quiet immobility (Fig. 5). In contrast, no such abnormalities were observed in control mice.

Alterations in background EEG is a frequent finding in mouse models of neurodevelopmental disorders (Sidorov et al., 2017; Wen et al., 2019). We next asked if there were significant differences in the background EEG between control and *Cdkl5* mutant mice. We conducted power spectral analysis using fast Fourier transforms (FFT), analyzing the light and dark periods of the 24 h cycle separately (Figs. 6 and 7). In the dark cycle, we found that both *Cdkl5*^{R59X}/+ and *Cdkl5*^{KO}/+ mice showed significantly increased power in the gamma frequency band (Fig. 6). In contrast, in the light cycle, we found that *Cdkl5*^{R59X}/+ mice again showed significantly increased power in the gamma frequency band. In addition, *Cdkl5*^{KO}/+ mice showed a significant decrease in power in the theta frequency band (Fig. 7).

4. Discussion

4.1. Epilepsy in mouse models of CDD

Here, we report and characterize, for the first time, epilepsy in two mouse models of CDD (*Cdkl5*^{R59X}/+ and *Cdkl5*^{KO}/+) using multichannel video-EEG recording. *Cdkl5* mutant mice recapitulated a major seizure type in CDD patients, the epileptic spasm, characterized by sudden-onset motor spasms associated with generalized slow-wave activity on EEG. Similar to CDD patients, there was significant variation in spasm burden in our mice. Furthermore, we found that spasms tend to occur in clusters during sleep and are associated with periods of elevated delta power and prominent interictal abnormalities. Finally, *Cdkl5* mutant mice also showed changes in overall background EEG power in the gamma and theta frequency bands.

In this study, epileptic spasms were the only type of spontaneous seizure detected in mutant mice during video-EEG monitoring. The spasms observed in *Cdkl5*^{R59X}/+ and *Cdkl5*^{KO}/+ mice were sudden-onset and brief, tended to occur in clusters during sleep, and were most often associated with slow-wave activity on the ictal EEG with the variable presence of electrodecrement, features that bear similarities to those of epileptic spasms in other mouse models (Dulla, 2018; Marsh et al., 2009; Marsh and Golden, 2009; Price et al., 2009).

During our blinded review of video-EEG data, a small number of events in wild type mice were scored as epileptic spasms (Fig. 3 and Materials and Methods). Although epileptic spasms have not been reported in aged C57BL/6 mice, it is possible that some wild type mice may infrequently exhibit myoclonic movements associated with synchronous electrographic activity. Alternatively, due to the prolonged duration of our study, it is possible that electrographic spikes, which are sometimes seen in C57BL/6 mice (Purtell et al., 2018), may infrequently coincide with brief body movements during sleep in a manner that can be interpreted as an epileptic event. Of note, the number of such spasms observed in the entire cohort of wild type mice is significantly smaller in comparison to the prominent spasm frequency seen in many *Cdkl5*^{R59X}/+ and *Cdkl5*^{KO}/+ mice. These data strongly suggest that epileptic spasms in the mutant mice are a specific phenomenon resulting from mutations in *Cdkl5*.

4.2. Epileptic spasms in aged Cdkl5 mutant mice

In CDD patients, epileptic spasms typically emerge during infancy or childhood (Bahi-Buisson et al., 2008a). Mouse models of epileptic spasms also tend to manifest these seizures at younger ages (Marsh and Golden, 2009). Therefore, the occurrence of epileptic spasms in aged *Cdkl5* mutant mice is an intriguing finding that stands in contrast with previous animal models. We believe that *Cdkl5* mutant mice could complement the existing models in several ways: 1) epileptic spasms are seen in a range of neurologic disorders and likely have diverse pathogenic mechanisms. *Cdkl5* mutant mice faithfully mimic the patient genetic lesion and can provide mechanistic insight into the pathways contributing to epileptic spasms. 2) Epileptic spasms can persist into adulthood, often as a manifestation of refractory epilepsy. Thus, *Cdkl5* mutant mice can be used for investigating the unique, adult-onset circuit disruptions that underlie this transition. 3) Epileptic spasms are often

associated with significant neurocognitive dysfunction, a behavioral deficit that is difficult to study early in life. *Cdkl5* mutant mice may provide a valuable opportunity to reveal a causal relationship between the emergence of seizures and cognitive decline.

The molecular pathogenic mechanisms that generate epilepsy in *Cdkl5* mutant mice remain unclear. Recent studies have revealed a role for excess NMDAR-dependent signaling in mediating specific behavioral deficits (Tang et al., 2019), and *Cdkl5* mutant mice are also distinctly susceptible to NMDA-induced generalized tonic-clonic seizures (Okuda et al., 2017). Interestingly, an established model of epileptic spasms, based on prenatal betamethasone administration, shows unique susceptibility to NMDA-induced spasms (Velíšek et al., 2007). Exploring the role of the brain-adrenal axis and NMDAR-dependent signaling, therefore, may reveal commonalities and differences between *Cdkl5* mutant mice and other existing models of epileptic spasms (Baram, 1993).

Whether seizures occur in younger *Cdkl5* mutant mice remains an important question. Multiple prior studies have failed to detect seizures in male *Cdkl5* mutant mice younger than 12–16 weeks of age (Amendola et al., 2014; Okuda et al., 2017; Wang et al., 2012). Young heterozygous female mice, however, have not been systemically studied using video-EEG recording, raising the possibility that epileptic spasms may emerge earlier in the life of *Cdkl5*^{R59X}/+ and *Cdkl5*^{KO}/+ mice. Furthermore, it is unknown whether aged hemizygous male mutant mice also shown epileptic spasms. Therefore, both the sex specificity and age-dependent progression of seizures in mouse models of CDD are important avenues of future investigation.

4.3. Interictal and background EEG abnormalities in Cdkl5 mutant mice

In multiple *Cdkl5*^{R59X}/+ and *Cdkl5*^{KO}/+ mice, we also observed prominent interictal abnormalities associated with clusters of epileptic spasms. The interictal abnormalities we find are reminiscent of the EEG features of CDD, including generalized polyspike and spike-wave activity. It is unclear why some, but not all, epileptiform discharges on EEG are associated with overt motor movements, a phenomenon also seen in patients. Therefore, mouse models of CDD could be used to investigate the potential mechanisms that underlie the electro-clinical dissociation between EEG spikes and motor spasms. Furthermore, interictal EEG is considered an important predictor of neurologic outcome in human patients with epileptic spasms (Kellaway et al., 1979). Thus, future studies should investigate the age at which interictal EEG abnormalities first emerge in the development of *Cdkl5* mutant mice and the extent to which they correlate with the onset of behavioral abnormalities, which have been reported in heterozygous female mice as early as 12–16 weeks of age (Fuchs et al., 2018). In the future, the presence of interictal abnormalities could serve as an added biomarker, alongside ictal events, in translational studies.

Of note, a common EEG feature of CDD and epileptic spasms that is absent in *Cdkl5* mutant mice is hypsarrhythmia, defined as high-voltage disorganized activity on EEG. Although hypsarrhythmia is considered a key feature for diagnosing epileptic spasms and West syndrome in human patients, it is rarely present in rodent models (Dulla, 2018; Marsh and Golden, 2009). Some of the reasons for this discrepancy include the lissencephalic nature of the rodent cortex and the smaller brain and skull size, which could make it difficult

to demonstrate clear organization (or lack thereof) on EEG. Thus, analogous interictal or background abnormalities in the rodent may manifest as other EEG patterns, such as high-amplitude epileptiform spiking.

Background EEG changes are a frequent finding in CDD and other neurodevelopmental disorders (Bahi-Buisson et al., 2008a; Wang et al., 2013) and has been reported in multiple mouse models of genetic epilepsy and neurodevelopmental disorders (Judson et al., 2016; Marsh et al., 2009; Sidorov et al., 2017). We discovered significant changes in the background EEG of *Cdkl5* mutant mice, specifically decreased power in the theta frequency band and increased power in the gamma frequency band, changes that were not seen in younger male *Cdkl5* mutant mice (Wang et al., 2012). Interestingly, heightened gamma oscillations have been associated with interictal epileptiform activity in patients and may play a role in generating pathologic network activity (Ren et al., 2015). On the other hand, loss of normal theta rhythmicity is seen in temporal lobe epilepsy and has been proposed as a possible cause of cognitive impairment (Shuman et al., 2017). Therefore, one interpretation of these background changes is that they may be critical in modulating the excitability of the brain, leading to periods of seizure susceptibility. Alternatively, they may be relatively independent of epilepsy in CDD and be an important underlying mechanism for the cognitive and social comorbidities in CDD. For example, early changes in the background EEG may represent significant dysfunction of underlying neural circuits and networks and may have value as a potential predictive biomarker for the development cognitive and social dysfunction observed in CDD.

Supplementary Material

Refer to Web version on PubMed Central for supplementary material.

Acknowledgments

This work was supported the Intellectual and Developmental Disabilities Research Center (IDDRC) at CHOP/PENN U54HD086984 (E.D.M, Z.Z., and D.A.C.), R01NS102731 (D.A.C. and Z.Z.), T32GM007170 (S.T.), and F30NS100433 (S.T.).

References

Ahrens-Nicklas RC, Tecedor L, Hall AF, Lysenko E, Cohen AS, Davidson BL, Marsh ED, 2019. Neuronal network dysfunction precedes storage and neurodegeneration in a lysosomal storage disorder. JCI Insight 4, 145. 10.1172/jci.insight.131961.

Amendola E, Zhan Y, Mattucci C, Castroflorio E, Calcagno E, Fuchs C, Lonetti G, Silingardi D, Vyssotski AL, Farley D, Ciani E, Pizzorusso T, Giustetto M, Gross CT, 2014. Mapping pathological phenotypes in a mouse model of CDKL5 disorder. PLoS One 910.1371/journal.pone.0091613. (e91613–12).

Bahi-Buisson N, Kaminska A, Boddaert N, Rio M, Afenjar A, Gérard M, Giuliano F, Motte J, Héron D, Morel MAN, Plouin P, Richelme C, Portes Des V, Dulac O, Philippe C, Chiron C, Nabbout R, Bienvenu T, 2008a. The three stages of epilepsy in patients with CDKL5 mutations. Epilepsia 49, 1027–1037. 10.1111/j.1528-1167.2007.01520.x. [PubMed: 18266744]

Bahi-Buisson N, Nectoux J, Rosas-Vargas H, Milh M, Boddaert N, Girard B, Cances C, Ville D, Afenjar A, Rio M, Heron D, N'Guyen Morel MA, Arzimanoglou A, Philippe C, Jonveaux P, Chelly J, Bienvenu T, 2008b. Key clinical features to identify girls with CDKL5 mutations. Brain 131, 2647–2661. 10.1093/brain/awn197. [PubMed: 18790821]

Baram TZ, 1993. Pathophysiology of massive infantile spasms: perspective on the putative role of the brain adrenal axis. Ann. Neurol. 33, 231–236. 10.1002/ana.410330302. [PubMed: 8388675]

Bernardo P, Ferretti A, Terrone G, Santoro C, Bravaccio C, Striano S, Coppola A, Striano P, 2019. Clinical evolution and epilepsy outcome in three patients with CDKL5-related developmental encephalopathy. Epileptic Disord 21, 271–277. 10.1684/epd.2019.1071. [PubMed: 31225800]

Butler KM, da Silva C, Alexander JJ, Hegde M, Escayg A, 2017. Diagnostic yield from 339 epilepsy patients screened on a clinical gene panel. Pediatr. Neurol. 77, 61–66. 10.1016/j.pediatrneurol.2017.09.003. [PubMed: 29056246]

Demarest ST, Olson HE, Moss A, Pestana-Knight E, Zhang X, Parikh S, Swanson LC, Riley KD, Bazin GA, Angione K, Niestroj L-M, Lal D, Juarez-Colunga E, Benke TA, 2019. CDKL5 deficiency disorder: relationship between genotype, epilepsy, cortical visual impairment, and development. Epilepsia 60, 1733–1742. 10.1111/epi.16285. [PubMed: 31313283]

Dulla CG, 2018. Utilizing animal models of infantile spasms. Epilepsy Curr. 18, 107–112. 10.5698/1535-7597.18.2.107. [PubMed: 29670486]

Fallah MS, Eubanks JH, 2020. Seizures in mouse models of rare neurodevelopmental disorders. Neuroscience. 10.1016/j.neuroscience.2020.01.041.

Fehr S, Wong K, Chin R, Williams S, de Klerk N, Forbes D, Krishnaraj R, Christodoulou J, Downs J, Leonard H, 2016. Seizure variables and their relationship to genotype and functional abilities in the CDKL5 disorder. Neurology 87, 2206–2213. 10.1212/WNL.0000000000003352. [PubMed: 27770071]

Fuchs C, Gennaccaro L, Trazzi S, Bastianini S, Bettini S, Martire Lo V, Ren E, Medici G, Zoccoli G, Rimondini R, Ciani E, 2018. Heterozygous CDKL5 knockout female mice are a valuable animal model for CDKL5 disorder. Neural Plast 201810.1155/2018/9726950. (9726950–18).

Grosso S, Brogna A, Bazzotti S, Renieri A, Morgese G, Balestri P, 2007. Seizures and electroencephalographic findings in CDKL5 mutations: case report and review. Brain Dev. 29, 239–242. 10.1016/j.braindev.2006.09.001. [PubMed: 17049193]

Judson MC, Wallace ML, Sidorov MS, Burette AC, Gu Bin, van Woerden GM, King IF, Han JE, Zylka MJ, Elgersma Y, Weinberg RJ, Philpot BD, 2016. GABAergic neuron-specific loss of Ube3a causes Angelman syndrome-like EEG abnormalities and enhances seizure susceptibility. Neuron 90, 1–15. 10.1016/j.neuron.2016.02.040. [PubMed: 27054611]

Kahn JB, Port RG, Yue C, Takano H, Coulter DA, 2019. Circuit-based interventions in the dentate gyrus rescue epilepsy-associated cognitive dysfunction. Brain 142, 2705–2721. 10.1093/brain/awz209. [PubMed: 31363737]

Kellaway P, Hrachovy RA, Frost JD, Zion T, 1979. Precise characterization and quantification of infantile spasms. Ann. Neurol. 6, 214–218. 10.1002/ana.410060306. [PubMed: 534418]

Klein KM, Yendle SC, Harvey AS, Antony JH, Wallace G, Bienvenu T, Scheffer IE, 2011. A distinctive seizure type in patients with CDKL5 mutations: Hypermotortonic-spasms sequence. Neurology 76, 1436–1438. 10.1212/WNL.0b013e3182166e58. [PubMed: 21502606]

Lindy AS, Stosser MB, Butler E, Downtain-Pickersgill C, Shanmugham A, Retterer K, Brandt T, Richard G, McKnight DA, 2018. Diagnostic outcomes for genetic testing of 70 genes in 8565 patients with epilepsy and neurodevelopmental disorders. Epilepsia 59, 1062–1071. 10.1111/epi.14074. [PubMed: 29655203]

Marsh ED, Golden JA, 2009. Developing an animal model for infantile spasms: pathogenesis, problems and progress. Dis. Model. Mech. 2, 329–335. 10.1242/dmm.001883. [PubMed: 19553693]

Marsh E, Fulp C, Gomez E, Nasrallah I, Minarcik J, Sudi J, Christian SL, Mancini G, Labosky P, Dobyns W, Brooks-Kayal A, Golden JA, 2009. Targeted loss of Arx results in a developmental epilepsy mouse model and recapitulates the human phenotype in heterozygous females. Brain 132, 1563–1576. 10.1093/brain/awp107. [PubMed: 19439424]

Okuda K, Kobayashi S, Fukaya M, Watanabe A, Murakami T, Hagiwara M, Sato T, Ueno H, Ogonuki N, Komano-Inoue S, Manabe H, Yamaguchi M, Ogura A, Asahara H, Sakagami H, Mizuguchi M, Manabe T, Tanaka T, 2017. CDKL5 controls postsynaptic localization of GluN2B-containing NMDA receptors in the hippocampus and regulates seizure susceptibility. Neurobiol. Dis. 106, 158–170. 10.1016/j.nbd.2017.07.002. [PubMed: 28688852]

Okuda K, Takao K, Watanabe A, Miyakawa T, Mizuguchi M, Tanaka T, 2018. Comprehensive behavioral analysis of the Cdkl5 knockout mice revealed significant enhancement in anxiety- and fear-related behaviors and impairment in both acquisition and long-term retention of spatial reference memory. PLoS One 13, e0196587. 10.1371/journal.pone.0196587. [PubMed: 29702698]

Olson HE, Demarest ST, Pestana-Knight EM, Swanson LC, Iqbal S, Lal D, Leonard H, Cross JH, Devinsky O, Benke TA, 2019. Cyclin-dependent kinase-like 5 deficiency disorder: clinical review. Pediatr. Neurol. 97, 18–25. 10.1016/j.pediatrneurol.2019.02.015. [PubMed: 30928302]

Pintaudi M, Baglietto MG, Gaggero R, Parodi E, Pessagno A, Marchi M, Russo S, Veneselli E, 2008. Clinical and electroencephalographic features in patients with CDKL5 mutations: two new Italian cases and review of the literature. Epilepsy Behav. 12, 326–331. 10.1016/j.yebeh.2007.10.010. [PubMed: 18063413]

Price MG, Yoo JW, Burgess DL, Deng F, Hrachovy RA, Frost JD, Noebels JL, 2009. A Triplet Repeat Expansion Genetic Mouse Model of Infantile Spasms Syndrome, Arx(GCG)10+7, with Interneuronopathy, Spasms in Infancy, Persistent Seizures, and Adult Cognitive and Behavioral Impairment. 29. pp. 8752–8763. 10.1523/JNEUROSCI.0915-09.2009.

Purtell H, Dhamne SC, Gurnani S, Bainbridge E, Modi ME, Lammers SHT, Super CE, Hameed MQ, Johnson EL, Sahin M, Rotenberg A, 2018. Electrographic spikes are common in wildtype mice. Epilepsy Behav. 89, 94–98. 10.1016/j.yebeh.2018.09.003. [PubMed: 30399547]

Ren L, Kucewicz MT, Cimbalnik J, Matsumoto JY, Brinkmann BH, Hu W, Marsh WR, Meyer FB, Stead SM, Worrell GA, 2015. Gamma oscillations precede interictal epileptiform spikes in the seizure onset zone. Neurology 84, 602–608. 10.1212/WNL.0000000000001234. [PubMed: 25589669]

Shuman T, Amendolara B, Golshani P, 2017. Theta rhythmopathy as a cause of cognitive disability in TLE. Epilepsy Curr. 17, 107–111. 10.5698/1535-7511.17.2.107. [PubMed: 28491003]

Sidorov MS, Deck GM, Dolatshahi M, Thibert RL, Bird LM, Chu CJ, Philpot BD, 2017. Delta rhythmicity is a reliable EEG biomarker in Angelman syndrome: a parallel mouse and human analysis. J. Neurodev. Disord 910.1186/s11689-017-9195-8. (17–14).

Simonet JC, Sunnen CN, Wu J, Golden JA, Marsh ED, 2015. Conditional loss of Arx from the developing dorsal telencephalon results in behavioral phenotypes resembling mild human ARX mutations. Cereb. Cortex 25, 2939–2950. 10.1093/cercor/bhu090. [PubMed: 24794919]

Symonds JD, Zuberi SM, Stewart K, McLellan A, O'Regan M, MacLeod S, Jollands A, Joss S, Kirkpatrick M, Brunklaus A, Pilz DT, Shetty J, Dorris L, Abu-Arafeh I, Andrew J, Brink P, Callaghan M, Cruden J, Diver LA, Findlay C, Gardiner S, Grattan R, Lang B, MacDonnell J, McKnight J, Morrison CA, Nairn L, Slean MM, Stephen E, Webb A, Vincent A, Wilson M, 2019. Incidence and phenotypes of childhood-onset genetic epilepsies: a prospective population-based national cohort. Brain 142, 2303–2318. 10.1093/brain/awz195. [PubMed: 31302675]

Takeda K, Miyamoto Y, Yamamoto H, Ishii A, Hirose S, Yamamoto H, 2020. Clinical features of early myoclonic encephalopathy caused by a CDKL5 mutation. Brain Dev. 42, 73–76. 10.1016/j.braindev.2019.08.003. [PubMed: 31492455]

Tang S, Terzic B, Wang I-TJ, Sarmiento N, Sizov K, Cui Y, Takano H, Marsh ED, Zhou Z, Coulter DA, 2019. Altered NMDAR signaling underlies autistic-like features in mouse models of CDKL5 deficiency disorder. Nat. Commun. 10, 2655. 10.1038/s41467-019-10689-w. [PubMed: 31201320]

Velíšek L, Jehle K, Asche S, Velíšková J, 2007. Model of infantile spasms induced by N-methyl-D-aspartic acid in prenatally impaired brain. Ann. Neurol. 61, 109–119. 10.1002/ana.21082. [PubMed: 17315208]

Wang I-TJ, Allen M, Goffin D, Zhu X, Fairless AH, Brodkin ES, Siegel SJ, Marsh ED, Blendy JA, Zhou Z, 2012. Loss of CDKL5 disrupts kinome profile and event-related potentials leading to autistic-like phenotypes in mice. Proc. Natl. Acad. Sci. U. S. A. 109, 21516–21521. 10.1073/pnas.1216988110. [PubMed: 23236174]

Wang J, Barstein J, Ethridge LE, Mosconi MW, Takarae Y, Sweeney JA, 2013. Resting state EEG abnormalities in autism spectrum disorders. J. Neurodev. Disord 510.1186/1866-1955-5-24. (24–14).

Wen TH, Lovelace JW, Ethell IM, Binder DK, Razak KA, 2019. Developmental changes in EEG phenotypes in a mouse model of fragile X syndrome. Neuroscience 398, 126–143. 10.1016/j.neuroscience.2018.11.047. [PubMed: 30528856]

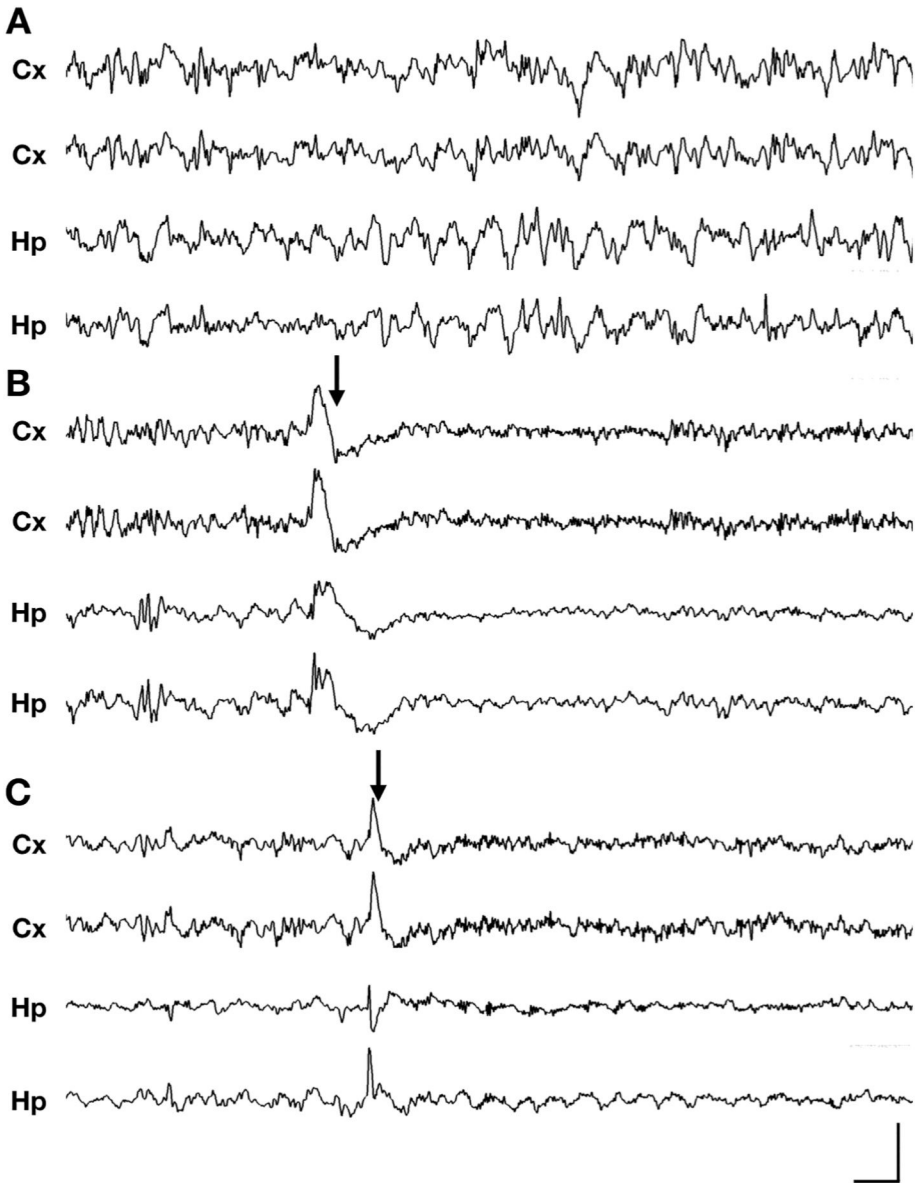

Fig. 1. Epileptic spasms in aged *Cdkl5* mutant heterozygous female mice.

(A-C) Representative 10-s traces of intracranial EEG recorded in wild type (+/+), *Cdkl5*^{R59X}/+, and *Cdkl5*^{KO}/+ heterozygous mice (Cx, cortical; Hp, hippocampal). (A) Normal EEG during sleep in a wild type mouse, showing intermittent delta rhythm. (B) Epileptic spasm in a *Cdkl5*^{R59X}/+ heterozygous female mouse occurring during sleep, characterized by bilateral slow-wave activity followed by an electrodecrement pattern. See also Supplementaary Video 1. (C) Epileptic spasm in a *Cdkl5*^{KO}/+ heterozygous female mouse occurring during sleep, characterized by bilateral sharp-wave activity. No clear electrodecrement is associated with this ictal event. See also Supplementary Video 2. (A-C) Vertical scale bar represents 1 mV, 800 μV, and 1.5 mV in cortical channels, respectively, and 500 μV, 800 μV, and 1 mV in hippocampal channels in, respectively. Horizontal scale bar represents 0.5 s in all traces. (–eC) Arrows indicate time of spasm

onset. Additional spasm-associated ictal events in *Cdkl5*^{R59X}/+ and *Cdkl5*^{KO}/+ mice are presented in Supplementary Fig. 1.

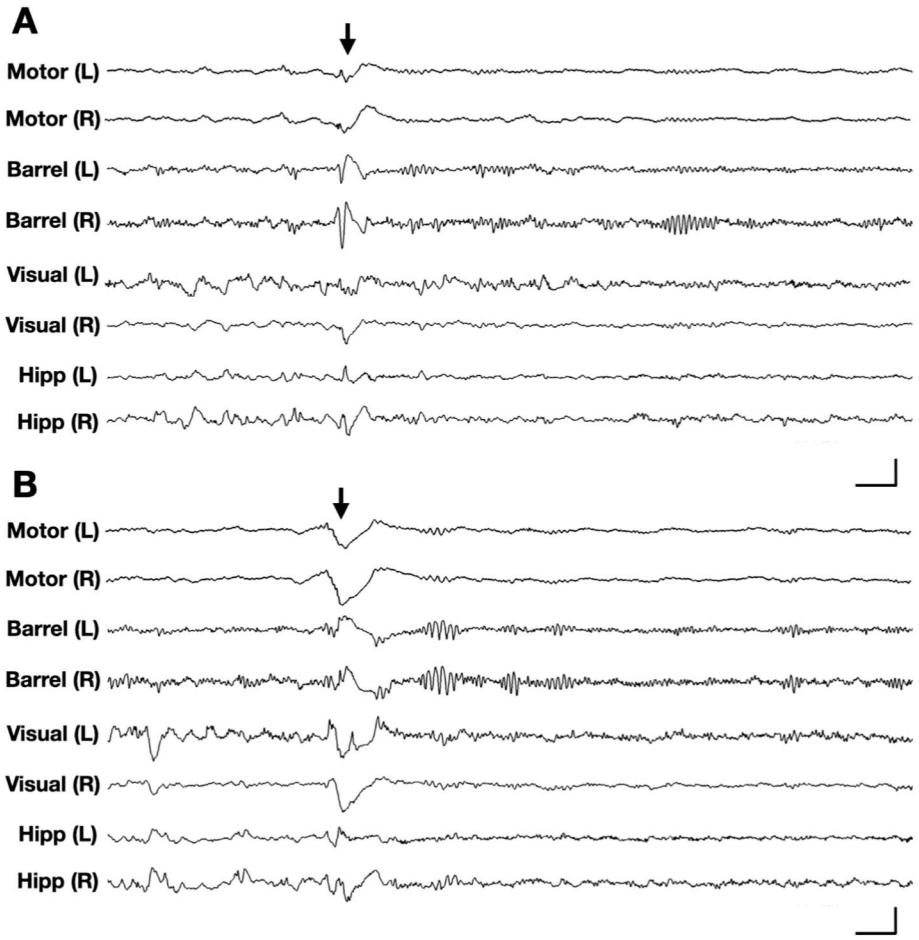

Fig. 2. Generalized epileptic spasms in *Cdkl5*^{KO}/+ mice.

Representative 5-s traces of 8-channel intracranial EEG (channels: left/right motor cortex, barrel cortex, visual cortex, and hippocampus) recorded in a *Cdkl5*^{KO}/+ mouse. (A) EEG corresponding to an epileptic spasm in a *Cdkl5*^{KO}/+ mouse during sleep, characterized by bilaterally symmetric onset, spike-wave activity in barrel cortices and slow-wave activity in motor cortices. (B) EEG corresponding to another epileptic spasm in the same *Cdkl5*^{KO}/+ mouse, several minutes later. This event is characterized by bilaterally symmetric onset, slow-wave activity in the motor and barrel cortices. (A-B) Vertical scale bars represent 1.8 mV, 1 mV, 1 mV, and 500 μV in bilateral motor cortex, barrel cortex, visual cortex, and hippocampal channels, respectively. Horizontal scale bars represent 0.25 s. Arrows indicate time of spasm onset.

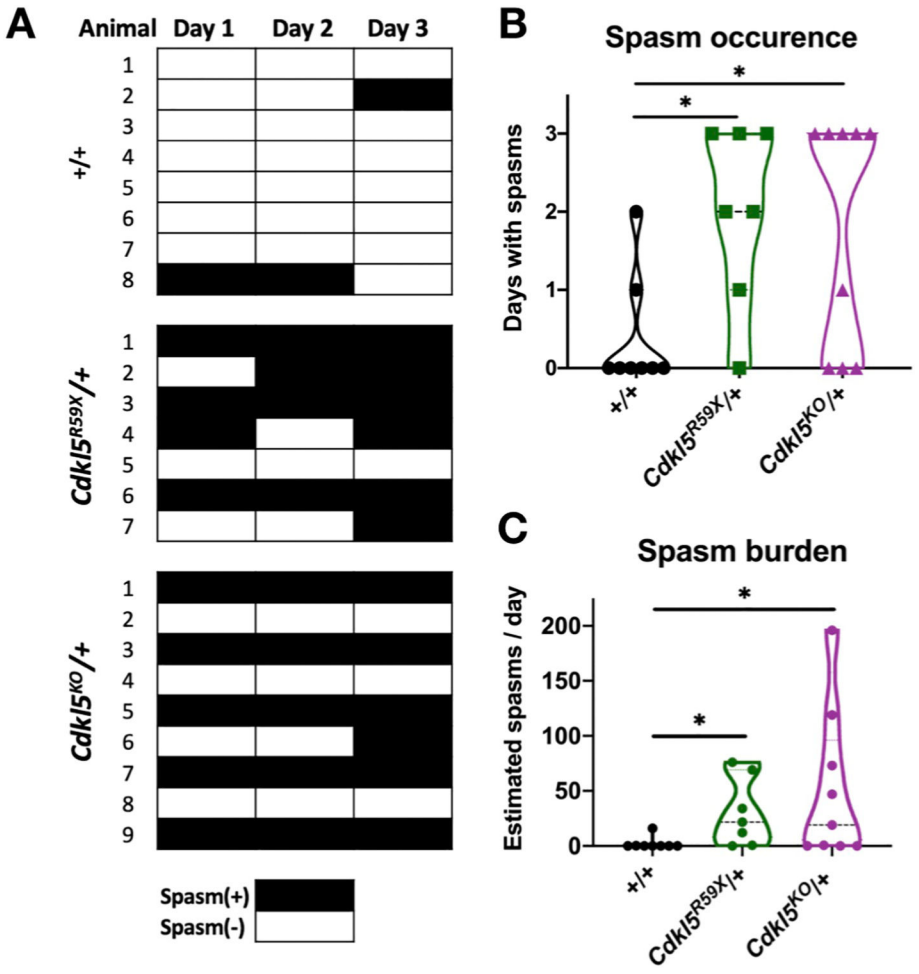

Fig. 3. Epileptic spasms occur with variable frequency in *Cdkl5* mutant mice.

(A) Occurrence of epileptic spasms in +/+ ($n = 8$), *Cdkl5*^{R59X}/+ ($n = 7$), and *Cdkl5*^{KO}/+ ($n = 9$) mice over three days. Black boxes indicate days with one or more detected epileptic spasms. (B) Comparison of spasm occurrence over three days in +/+, *Cdkl5*^{R59X}/+, and *Cdkl5*^{KO}/+ mice. For each mouse, the number of days (out of three total days) with one or more epileptic spasms was quantified. Mann-Whitney tests with Holm's correction for multiple comparisons (+/+ vs *Cdkl5*^{R59X}/+, $p = .018$; +/+ vs *Cdkl5*^{KO}/+, $p = .023$). (C) Estimated daily spasm burden is compared across +/+, *Cdkl5*^{R59X}/+, and *Cdkl5*^{KO}/+ mice. For each mouse, spasms were counted for a randomly selected day. Mann-Whitney tests with Holm's correction for multiple comparisons (+/+ vs *Cdkl5*^{R59X}/+, $p = .011$; +/+ vs *Cdkl5*^{KO}/+, $p = .019$).

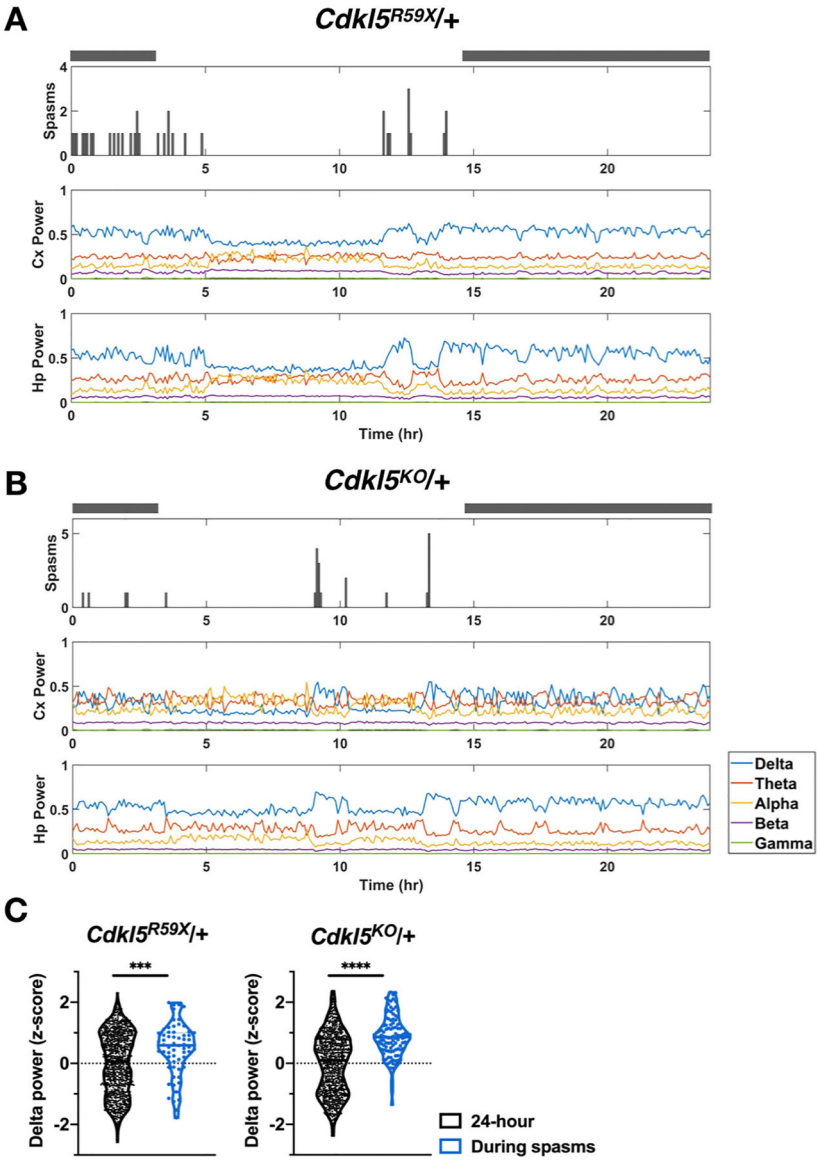

Fig. 4. Epileptic spasms in *Cdkl5* mutant mice often occur in clusters during episodes of high delta power.

(A) Raster plot for epileptic spasms for a $Cdkl5^{R59X/+}$ mouse, showing clustering of spasms and preferential occurrence during periods of elevated delta power in both cortical and hippocampal channels. Grey bars above plots indicate the dark cycle. Spasms and delta power were quantified in five-minute epochs. (B) Similar plot as in (A) for a $Cdkl5^{KO/+}$ mouse. (C) Comparison of delta power values during spasms vs. during the enclosing 24 h period. For each mouse, delta power z-scores were calculated for each five-minute epoch. The distribution of z-scores during spasms was then compared to the overall distribution during enclosing 24 h period. $Cdkl5^{R59X/+}$ and $Cdkl5^{KO/+}$ mice show significantly increased delta power during epochs with spasms ($n = 3$ mice per genotype). Kolmogorov-Smirnov tests ($Cdkl5^{R59X/+}$, $p = .0005$; $Cdkl5^{KO/+}$, $p < .0001$).

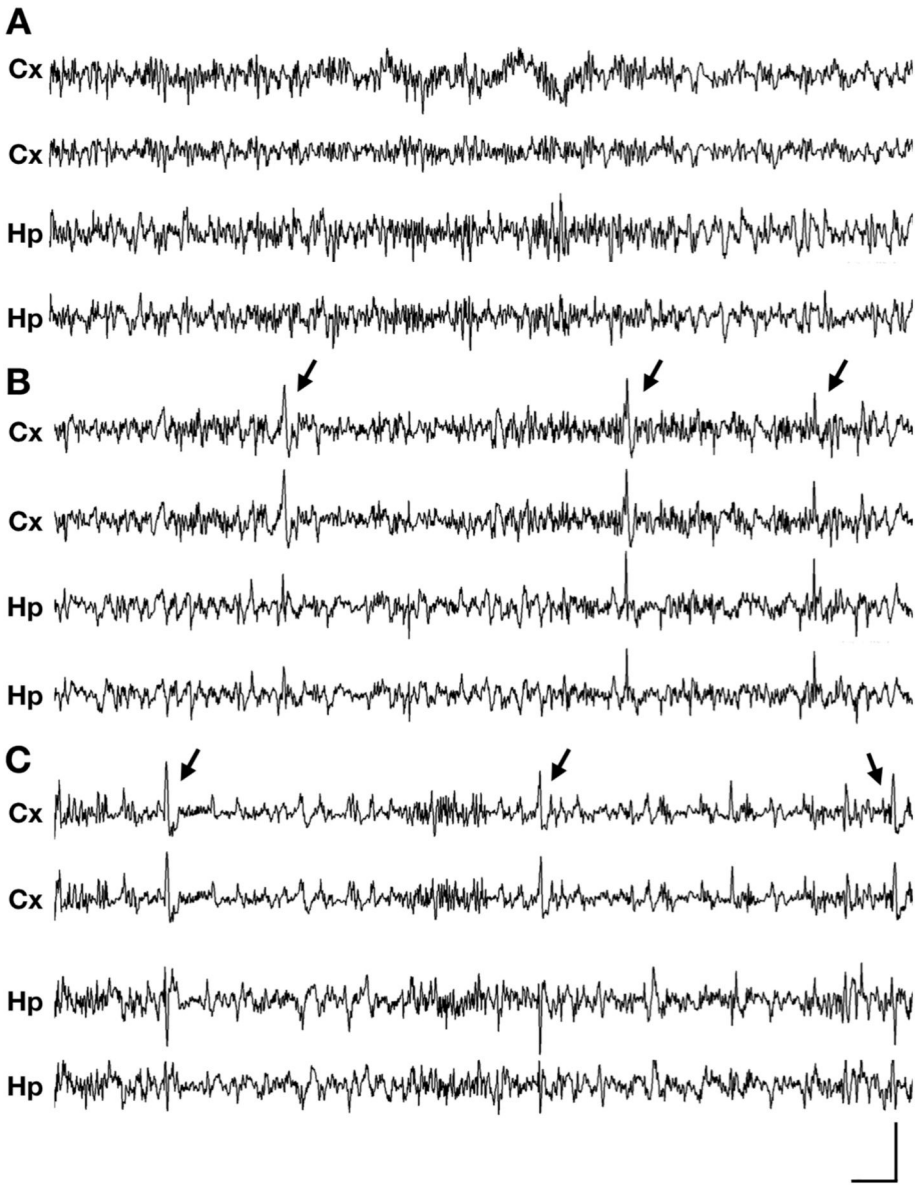

Fig. 5. Interictal abnormalities on EEG in *Cdkl5* mutant mice.

(A-C) Representative 30 s traces of intracranial EEG recorded in wild type and *Cdkl5* mutant heterozygous mice (Cx, cortical; Hp, hippocampal). (A) Normal background during sleep in a wild type (+/+) mouse. (B) Interictal spiking during a period of behavioral arrest in a $Cdkl5^{R59X}$/+. (C) Interictal spiking during a period of behavioral arrest in a $Cdkl5^{KO}$/+ mouse. (A-C) Vertical scale bar represents 1.5 mV, 1.2 mV, and 1.5 mV in cortical channels, respectively, and 600 μV, 600 μV, and 400 μV in hippocampal channels, respectively. Horizontal scale bar represents 1.5 s in all traces. Arrows indicate interictal spikes.

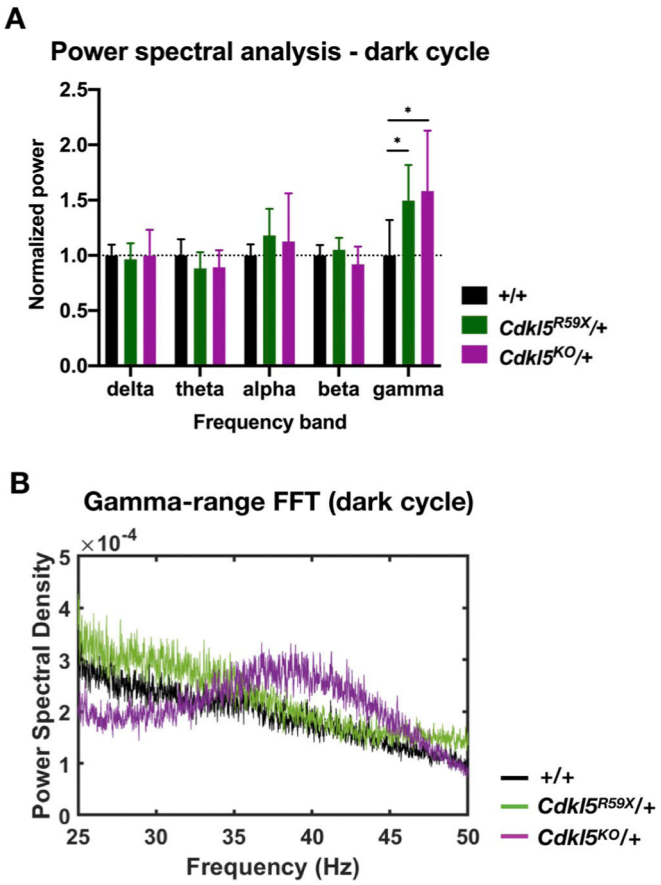

Fig. 6. Changes in background EEG in *Cdkl5* mutant mice during the dark cycle.

(A) Comparison of normalized power in various frequency bands in +/+, *Cdkl5*^{R59X}/+, and *Cdkl5*^{KO}/+ mice during the dark cycle. For each mouse, 10 randomly selected, 10 min bins were selected and averaged. Two-way ANOVA with Dunnett's multiple comparisons test (effect of interaction between frequency band and genotype, $p = .0064$; +/+ vs *Cdkl5*^{R59X}/+ gamma band power, p = .019; +/+ vs *Cdkl5*^{KO}/+ gamma band power, $p = .032$). (B) Representative FFTs in the gamma range (25–50 Hz) for +/+, *Cdkl5*^{R59X}/+, and *Cdkl5*^{KO}/+ mice during the dark cycle. Note the elevated gamma band power in *Cdkl5*^{R59X}/+ and *Cdkl5*^{KO}/+ mice, relative to +/+. Sample FFTs in (B) were smoothed using a 25-point function.

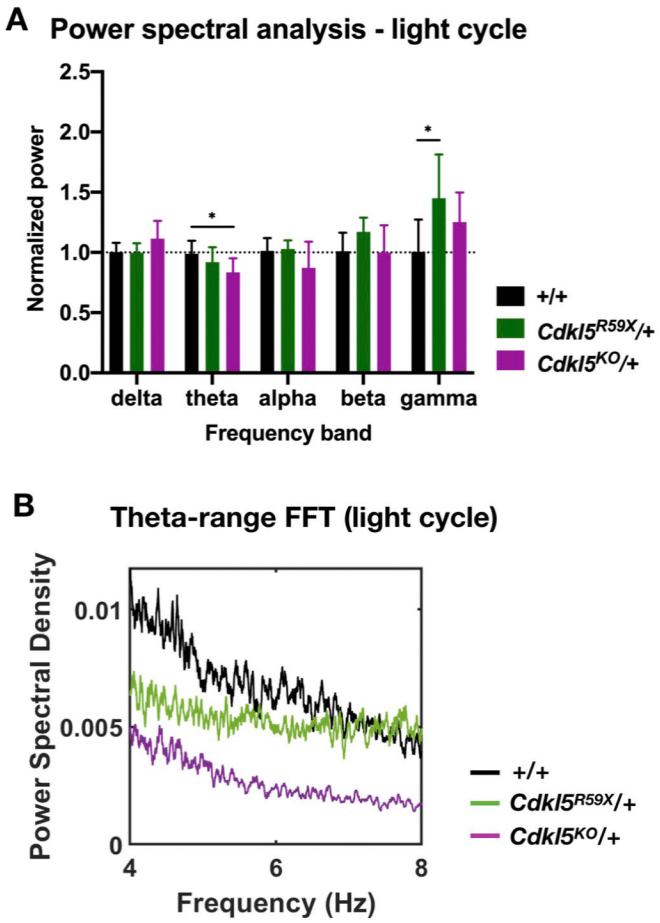

Fig. 7. Changes in background EEG in *Cdkl5* mutant mice during the light cycle.

(A) Comparison of normalized power in various frequency bands in +/+, *Cdkl5*^{R59X}/+, and *Cdkl5*^{KO}/+ mice during the light cycle. For each mouse, 10 randomly selected, 10 min bins were selected and averaged. Two-way ANOVA with Dunnett's multiple comparisons test (effect of interaction between frequency band and genotype, p = .0064; +/+ vs *Cdkl5*^{KO}/+ theta band power, $p = .022$; +/+ vs *Cdkl5*^{R59X}/+ gamma band power, $p = .039$). (B) Representative FFT in the theta range (4–8 Hz) for +/+, *Cdkl5*^{R59X}/+, and *Cdkl5*^{KO}/+ mice during the light cycle. Note the decreased theta band power in *Cdkl5*^{KO}/+ mice, relative to +/+. Sample FFTs in (B) were smoothed using a 25-point function.